# Fatty Acid Hydroperoxides and $H_2O_2$ in the Execution of Hypersensitive Cell Death in Tobacco Leaves[1][w]

**Jean-Luc Montillet, Sangpen Chamnongpol[2], Christine Rustérucci[3], James Dat[4], Brigitte van de Cotte, Jean-Pierre Agnel, Christine Battesti, Dirk Inzé, Frank Van Breusegem, and Christian Triantaphylidès***

Commissariat à l'Energie Atomique/Cadarache, Direction des Sciences du Vivant, Département d'Ecophysiologie Végétale et de Microbiologie, Laboratoire de Radiobiologie Végétale, F–13108 Saint-Paul-Lez-Durance cedex, France (J.-L.M., C.R., J.-P.A., C.B., C.T.); and Department of Plant Systems Biology, Flanders Interuniversity Institute for Biotechnology, Ghent University, B–9052 Ghent, Belgium (S.C., J.D., B.v.d.C., D.I., F.V.B.)

We initially compared lipid peroxidation profiles in tobacco (*Nicotiana tabacum*) leaves during different cell death events. An upstream oxylipin assay was used to discriminate reactive oxygen species (ROS)-mediated lipid peroxidation from 9- and 13-lipoxygenase (LOX)-dependent lipid peroxidation. Free radical-mediated membrane peroxidation was measured during $H_2O_2$-dependent cell death in leaves of catalase-deficient plants. Taking advantage of these transgenic plants, we demonstrate that, under light conditions, $H_2O_2$ plays an essential role in the execution of cell death triggered by an elicitor, cryptogein, which provokes a similar ROS-mediated lipid peroxidation. Under dark conditions, however, cell death induction by cryptogein was independent of $H_2O_2$ and accompanied by products of the 9-LOX pathway. In the hypersensitive response induced by the avirulent pathogen *Pseudomonas syringae* pv *syringae*, both 9-LOX and oxidative processes operated concurrently, with ROS-mediated lipid peroxidation prevailing in the light. Our results demonstrate, therefore, the tight interplay between $H_2O_2$ and lipid hydroperoxides and underscore the importance of light during the hypersensitive response.

Different defense mechanisms are used by plants to cope with pathogen assaults. A major source of resistance is conditioned by the interaction between plant resistance and pathogen avirulence gene products (Martin et al., 2003; Rathjen and Moffett, 2003). This defense strategy is characterized by (1) the activation of the hypersensitive response (HR), typified by a localized programmed cell death activation; (2) the initiation of defense responses, including cell wall reinforcement, accumulation of phytoalexins, and expression of antimicrobial proteins; and (3) the onset of a local and systemic acquired resistance (Lamb and Dixon, 1997; Beers and McDowell, 2001; Greenberg and Yao, 2004).

The signaling cascades leading to the HR are starting to be elucidated. Several resistance genes have been cloned, and protein kinases, phosphatases, and GTP-binding proteins have all been implicated downstream of these recognition proteins (Martin et al., 2003; Rathjen and Moffett, 2003). Changes in ion fluxes across the plasma membrane and the production of reactive oxygen species (ROS) and nitric oxide (NO) are among the earliest events following pathogen infection or elicitor treatment in cultured plant cells (Doke, 1997; Grant and Loake, 2000; Wendehenne et al., 2004). The production of ROS is biphasic, with a sustained second oxidative burst in response to an avirulent pathogen, and monophasic and transient with a virulent pathogen. This suggests that ROS production may be responsible for some of the defense-associated processes (Lamb and Dixon, 1997). Furthermore, ROS, and specifically $H_2O_2$, are key modulators of NO in triggering plant cell death (Delledonne et al., 2001; Neill et al., 2002; Wendehenne et al., 2004).

In order to obtain further insight into the role of $H_2O_2$ in plant signaling and cell death, we used transgenic tobacco (*Nicotiana tabacum*) plants (Cat1AS), which only express 10% of wild-type catalase activity. CAT1 is the dominant catalase isoform in leaves, where it serves in the removal of photorespiratory-derived $H_2O_2$ (Willekens et al., 1997). Cat1AS plants are phenotypically very similar to wild-type plants when grown under low-light (LL) conditions, and variable in planta $H_2O_2$ concentrations may be achieved by modulating light intensities (Dat et al., 2003). This experimental model was previously used to mimic

[1] This work was supported by the Research Fund of the Ghent University (Geconcerteerde Onderzoeksacties; grant no. 12051403) and by an individual Marie Curie postdoctoral fellowship of the European Union (to J.D.).

[2] Present address: Panomics, Inc., 2003 East Bayshore Road, Redwood City, CA 94063.

[3] Present address: Laboratoire de Génomique Fonctionnelle des Plantes, Faculté des Sciences–Ilot des Poulies, 33 Rue St. Leu, F–80039 Amiens cedex, France.

[4] Present address: Laboratoire de Biologie Environnementale EA3184-usc, Institut National de la Recherche Agronomique, Université de Franche-Comté, Place Leclerc, F–25030 Besançon, France.

* Corresponding author; e-mail ctriantaphylid@cea.fr; fax 33–4–42–25–26–25.

[w] The online version of this article contains Web-only data.

Article, publication date, and citation information can be found at www.plantphysiol.org/cgi/doi/10.1104/pp.105.059907.

a sustained oxidative burst, allowing the role of $H_2O_2$ in ethylene and salicylic acid production to be pinpointed, as well as pathogenesis-related protein accumulation (Chamnongpol et al., 1998; Dat et al., 2001). In addition, pathogen infection of Cat1AS plants or transgenic tobacco plants with reduced ascorbate peroxidase activity demonstrated the direct involvement of $H_2O_2$ in limiting pathogen spread and suggested its participation in HR cell death (Mittler et al., 1999). More recently, using Cat1AS tobacco plants and modulating light intensity, we showed evidence of the role of $H_2O_2$ in triggering cell death in tobacco (Dat et al., 2003). A genome-wide transcriptome analysis revealed that a sustained $H_2O_2$ stress in Cat1AS plants mimicked the molecular response reported for biotic and abiotic stresses, including cell death (Vandenabeele et al., 2003). In this study, we aimed to obtain additional insight into the role of $H_2O_2$ in the execution phase of plant cell death.

In addition to the involvement of oxidative stress, cytochrome c release, and the activation of nucleases and proteases during plant cell death execution, we have proposed additional executioners involved in leaf HR cell death, which find their origin in the catabolism of membranes (Rustérucci et al., 1999; Lam, 2004). We showed that a 9-lipoxygenase (LOX)-dependent massive production of free fatty acid hydroperoxides operated during cryptogein-induced HR in tobacco. This process involves both galactolipase and 9-LOX activities targeting chloroplastic lipids (Cacas et al., 2005). This active lipid peroxidation is sufficient to induce plant cell death. Using antisense constructs, 9-LOX was shown as being essential in preventing further pathogen invasion in tobacco (Rancé et al., 1998). The 9-LOX metabolism is rapidly activated during incompatible plant-pathogen interactions, whereas it is delayed and reduced in compatible interactions (Jalloul et al., 2002; Montillet et al., 2002; Vailleau et al., 2002). A LOX-dependent programmed cell death was also shown on lentil (*Lens culinaris*) root protoplasts treated with $H_2O_2$ (Maccarone et al., 2000) and application of fatty acid hydroperoxides to tomato (*Lycopersicon esculentum*) protoplasts leads to all features of programmed cell death (Knight et al., 2001).

We have recently established an oxylipin profile of Arabidopsis (*Arabidopsis thaliana*) and shown that it is possible to discriminate 9-LOX-dependent, 13-LOX-dependent, and ROS-mediated lipid peroxidation (Montillet et al., 2004). Using such a profile, we assessed the modulation of the 9-oxylipin metabolism during tobacco HR and showed that, in cryptogein-elicited leaves, light inhibits both 9-LOX oxylipin metabolism and HR cell death (Cacas et al., 2005). In contrast, in Ralstonia-infected leaves, the HR is characterized by both 9-LOX-dependent and ROS-mediated lipid peroxidation. To date, ROS-mediated lipid peroxidation is assumed to reflect the production of $H_2O_2$; however, this has never been clearly assessed. Thus, we decided to directly assess the interplay between $H_2O_2$ and lipid hydroperoxide production and their relationship with plant cell death. Cat1AS tobacco plants were used as a model system (Dat et al., 2001) to compare pathogen- and elicitor-induced HR under variable $H_2O_2$ background levels. For this, cell death phenology and lipid peroxidation processes were monitored following sustained $H_2O_2$ stress, cryptogein application, or *Pseudomonas syringae* pv *syringae* infection. This allowed us to assess whether $H_2O_2$ is only involved in early signal transduction or is also involved in the execution of cell death during the HR. In addition, we address the importance of light in the development of HR cell death.

## RESULTS

### Oxidative Stress-Induced and HR Cell Death Phenology Is Different

We first compared the cell death phenology induced by a sustained $H_2O_2$ stress in Cat1AS tobacco plants with that provoked in plants infected with an avirulent pathogen. Therefore, all plants were pregrown in a 14/10-h day/night cycle at LL (100 $\mu$mol $m^{-2}$ $s^{-1}$ fluence rate), and both treatments were initiated at the start of the day. Cat1AS plants were exposed to high-light (HL) stress (350 $\mu$mol $m^{-2}$ $s^{-1}$ fluence rate), resulting in the increased production of photorespiratory $H_2O_2$ as described earlier (Willekens et al., 1997; Dat et al., 2003). In a parallel experiment, tobacco wild-type plants were inoculated with $10^7$ cfu $mL^{-1}$ of *P. syringae* pv s*yringae*. The first signs of leaf injury appeared in HL-exposed Cat1AS plants within 12 h, although bleached lesions only became prominent after 36 h (Fig. 1B). By then, all palisade parenchyma cells had collapsed, while both the upper and lower epidermal cell layer and most of the spongy parenchyma cells remained macroscopically untouched (Fig. 1F). In contrast, in pathogen-infected tobacco leaves exposed to HL, all cell layers were destroyed within 24 h (Fig. 1, C and G). This was also reflected by the complete dehydration of the infected leaf segments. In the light, symptom development was also characterized by bleaching (Fig. 1C), a phenotype not observed for infection in the dark, however, which also leads to complete dehydration (Fig. 1D).

Cell death phenology was also investigated in cryptogein-induced HR. Cryptogein primarily induces all the features leading in fine to HR cell death, including the oxidative burst, which is mainly characterized by the extracellular production of $H_2O_2$ (Simon-Plas et al., 1997). Cryptogein was applied to detached tobacco wild-type leaves from plants previously grown at LL, followed by continuous darkness (Fig. 1H) or by different light regimes at HL (12/12-h day/night regime for 48 h, Fig. 1I; 12/12-h night/day regime and continuous light for 48 h; data not shown). In the dark, HR symptoms appeared after 12 h and developed within 22 h, as expected, while in all the light regimes the onset of symptoms was significantly

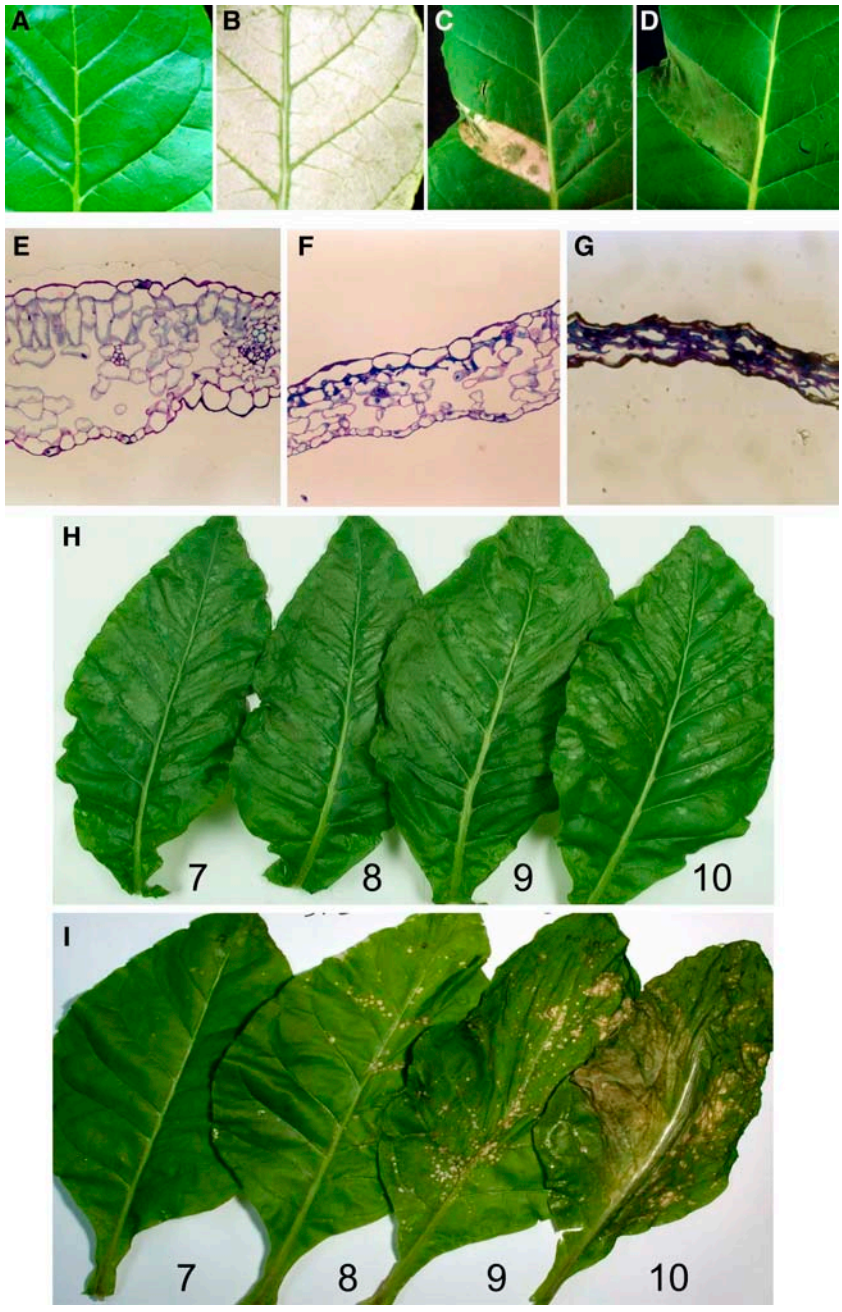


**Figure 1.** Leaf symptoms induced by HL in catalase-deficient tobacco (Cat1AS) and by pathogen infection or cryptogein application to wild-type tobacco leaves. All plants were grown at LL (100 $\mu$mol $m^{-2}$ $s^{-1}$ fluence rate) in a 14/10-h day/night cycle. A to G, Cat1AS tobacco plants were transferred to HL conditions (350 $\mu$mol $m^{-2}$ $s^{-1}$ fluence rate) at the beginning of the day; for comparison, Pseudomonas-inoculated wild types were transferred similarly to HL. A, Control leaf of Cat1AS plant. B, Leaf of Cat1AS plant exposed to HL for 31 h. C, Necrotic symptoms of Pseudomonas-inoculated wild-type leaf exposed to HL for 31 h. D, Same as in C, but incubation in complete darkness; Pseudomonas inoculation ($10^7$ cfu $mL^{-1}$) was carried out between two secondary leaf veins on the left part of the leaf and mock inoculation on the right part. E to G, Microscopic photographs of leaf sections corresponding to leaves shown in A to C, respectively. While completely bleached (B), the Cat1AS leaf showed absence of tissue collapse (F), whereas the infected wild-type leaf (C and D) displayed complete tissue dehydration (G). H and I, Cryptogein (10 $\mu$L at 0.2 $\mu$g $\mu L^{-1}$) was applied to the petiole of excised leaves at the end of the night period and then incubated in the dark for 22 h (H) or at HL in a day/night regime of 12/12 for 48 h (I). For I, the symptoms started appearing after 22 h (data not shown) and were fully developed within 48 h. H and I, Each photograph shows, from left to right, leaves from the same tobacco wild-type plant corresponding to the 7- to 10-leaf rank starting from the flower bud. The symptoms obtained in a night/day or continuous light regime were similar to those described in I. Photographs from one of two independent experiments are shown.

delayed (from approximately 10 h), starting after 22 h and leading to bleached spots within 48 h. Whereas in the light-treated leaves bleached spots are prominent (Fig. 1I), in the dark-treated leaves necrotic symptoms start to develop in the intervein areas and cover the leaf surface (Fig. 1H). In both cases, tissue dehydration is severe. A striking difference between the light and dark regimes is that, in the light, the appearance of cell death is noticeable only in the older leaves, whereas in the dark, no HR-induced cell death is noticeable between younger and older leaves.

A very similar cell death phenology as in the Pseudomonas- and cryptogein-induced HR was also observed within 24 h after (1) the infiltration of 1 M $H_2O_2$ in Cat1AS leaves in a continuous dark or normal day/night regime (LL); (2) a transient intense light exposure of Cat1AS plants (7 h at 1,000 $\mu$mol $m^{-2}$ $s^{-1}$ fluence rate), followed by continuous dark or a normal day/night regime at LL; and (3) the infiltration of the NO donor, sodium nitroprusside (SNP; 1–2 mM), in leaf segments of wild-type plants and incubation either in the dark or after a transient HL exposure (6 h) and dark (data not shown).

From these experiments, we can conclude that the cell death phenology provoked by a sustained $H_2O_2$ stress (phenotype I) and an avirulent pathogen

infection, cryptogein elicitation, or $H_2O_2$ and NO pulses (phenotype II) are clearly different. In phenotype I, cell death is restricted to the palisade layer, whereas in phenotype II, all cell layers collapse, leading to a total dehydration of the leaf. In the latter case, subsequent bleaching takes place in the light.

### $H_2O_2$ Stress Induces a Free Radical-Mediated Membrane Lipid Peroxidation Driven by Light

In order to investigate ROS-mediated lipid peroxidation in relation to $H_2O_2$ production, we took advantage of the Cat1AS plants and analyzed the effects of (1) increased production of photorespiratory $H_2O_2$ and (2) apoplastic infiltration of $H_2O_2$, both treatments leading to cell death symptoms (see above).

We assessed the kinetics of lipid peroxidation accumulation in both Cat1AS and wild-type plants transferred from LL to HL by HPLC analysis of the hydroxy fatty acids (HFAs), as previously described (Rustérucci et al., 1999). HFAs were hardly detectable in wild-type leaves but started to accumulate after 2 d of sustained $H_2O_2$ stress in Cat1AS leaves (Fig. 2A). Lipid peroxidation largely coincided with the appearance of bleaching, and HFA levels reached a plateau within 31 h (total hydroxy octadecatrienoic acids [HOTEs]; Fig. 2A, 1.3 $\mu$mol $g^{-1}$ dry weight [DW]; see Table I legend for HFA abbreviations). As the kinetics of accumulation of each positional HFA of both 18:2 (data not shown) and 18:3 (Fig. 2A) were identical and reached similar levels, this is most likely the result of a free radical-mediated lipid peroxidation instead of one catalyzed by an enzymatic process. Chiral phase HPLC analysis of each HFA showed that, in nonstressed wild-type and Cat1AS leaves as well as in stressed wild-type leaves, 13-hydroxy octadecadienoic acid (HODE) and 13-HOTE showed some *S*-specificity (Table I). This is indicative of a basal constitutive (13*S*)-LOX activity, as previously noticed (Rustérucci et al., 1999). In stressed Cat1AS leaves, all tested isomers were clearly racemic, confirming a free radical-mediated process (Table I). Additionally, we assessed membrane lipid peroxidation by analyzing free and esterified products of lipid peroxidation and the hydroperoxide formation using the volatile alkane assay (Degousée et al., 1995). We observed that at least 90% of HFAs are esterified and hydroperoxides accumulate at high levels, demonstrating membrane lipid peroxidation (see Supplemental Fig. 1). Lipid peroxidation was then investigated in leaves of wild-type and Cat1AS plants infiltrated with 1 M $H_2O_2$ and incubated either in the dark or in the light for 24 h. Both cell death and lipid peroxidation were absent on the infiltrated areas of wild-type leaves because endogenous catalase levels act as an efficient sink for the infiltrated $H_2O_2$ (data not shown; Willekens et al., 1997). In contrast, Cat1AS-infiltrated leaves developed cell death symptoms in the dark on about 40% of the infiltrated area together with lipid peroxidation (total HOTEs, 0.68 $\mu$mol $g^{-1}$ DW, as compared to 0.15 for controls). Moreover, in

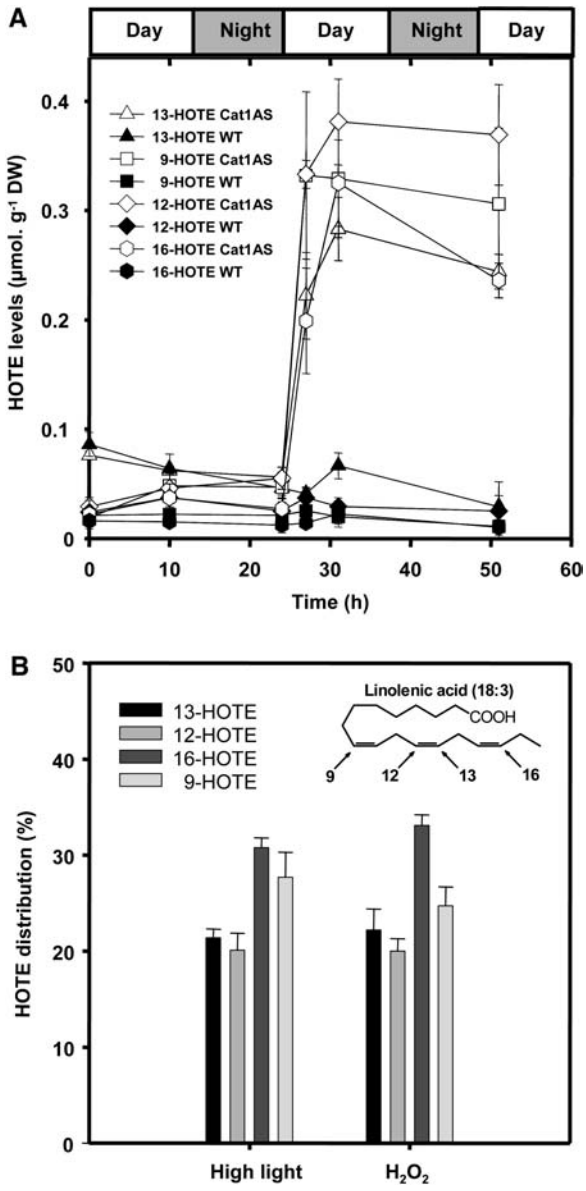


**Figure 2.** Lipid peroxidation in leaves of catalase-deficient transgenic (Cat1AS) and wild-type (WT) tobacco plants after transfer to HL. A, Kinetics of lipid peroxidation given for each specific isomer of 18:3 for Cat1AS and wild-type plants transferred to HL conditions (350 $\mu$mol $m^{-2}$ $s^{-1}$ fluence rate) at the beginning of the day (day/night, 14/10 h). Lipid hydroperoxides of leaf extracts are analyzed by HPLC as HFAs obtained by the $NaBH_4$ hydrolysis procedure. Results expressed as mean ± SD from three independent leaves. B, ROS-mediated isomer distribution for the HFAs of linolenic acid (18:3) in tobacco leaves. Inset, Peroxidation positions for 18:3. The isomer distribution for HL was obtained from the results described in A; results expressed as mean ± SD ($n$ = 9). The distribution for $H_2O_2$ was obtained from Cat1AS leaves infiltrated with 1 M $H_2O_2$ and incubated in a normal day/night regime (LL); the oxylipin signature associated with the necrotic symptoms was characterized after 24 h. Results expressed as mean ± SD ($n$ = 4). See Table I for abbreviations.

**Table I.** *Enantioselectivity in lipid peroxidation induced by HL and cryptogein*

Enantiomer composition of the HFAs obtained by the $NaBH_4$/hydrolysis procedure from leaves of wild-type and Cat1AS tobacco plants (1) transferred from LL (100 $\mu$mol $m^{-2}$ $s^{-1}$ fluence rate) to HL (350 $\mu$mol $m^{-2}$ $s^{-1}$ fluence rate) conditions and (2) elicited with cryptogein in combination or not with HL. The timing corresponds to fully developed symptoms. Results are expressed as mean ± SD ($n$ = 2). 9-HODE, 9-hydroxy-10,12(*E*,*Z*) octadecadienoic acid; 13-HODE, 13-hydroxy-9,11(*Z*,*E*) octadecadienoic acid; 9-HOTE, 9-hydroxy-10,12,15(*E*,*Z*,*Z*) octadecatrienoic acid; 12-HOTE, 12-hydroxy-9,13,15(*Z*,*E*,*Z*)-octadecatrienoic acid; 13-HOTE, 13-hydroxy-9,11,15(*Z*,*E*,*Z*)-octadecatrienoic acid; 16-HOTE, 16-hydroxy-9,12,14(*Z*,*Z*,*E*)-octadecatrienoic acid.

| HFAs | (*S*)-Enantiomer (%) | | | | |
|---|---|---|---|---|---|
| | Cat1AS LL (Day/Night, 14/10 h)[a] | Cat1AS HL, 31 h (Day/Night, 14/10 h)[b] | Wild Type; Cryptogein, Dark, 30 h | Wild Type; Cryptogein, Continuous HL, 48 h | Cat1AS; Cryptogein, Continuous HL, 22 h |
| 9-HODE | 51 ± 8 | 50 ± 1 | 87 ± 2 | 63 ± 4 | 65 ± 2 |
| 9-HOTE | 48 ± 1 | 50 ± 1 | 90 ± 2 | 62 ± 6 | 69 ± 1 |
| 13-HODE | 79 ± 5 | 50 ± 1 | 70 ± 3 | 59 ± 1 | 51 ± 1 |
| 13-HOTE | 87 ± 6 | 50 ± 1 | 82 ± 2 | 63 ± 4 | 49 ± 1 |
| 12-HOTE | 51 ± 5 | 51 ± 2 | 52 ± 2 | 53 ± 2 | 50 ± 1 |
| 16-HOTE | 53 ± 5 | 50 ± 1 | 55 ± 3 | 50 ± 3 | 52 ± 2 |

[a]Wild type at LL and HL, as well as Cat1AS in the dark, gave similar enantiomeric distributions. [b]Cat1AS leaves infiltrated with 1 M $H_2O_2$ and incubated at LL gave the same racemic enantiomeric composition.

a day/night cycle at LL, this process was increased 10-fold (6.7 $\mu$mol $g^{-1}$ DW), with cell death symptoms covering the entire infiltrated area. Interestingly, the HOTE isomer distribution is randomized and similar to the distribution obtained following a sustained $H_2O_2$ stress in HL-treated Cat1AS plants (see Fig. 2B for comparison). Such randomized HOTE isomer and enantiomer distribution (Table I) is again a marker of a free radical-mediated lipid peroxidation process (Montillet et al., 2004).

### Cell Death Is Not Always Associated with Lipid Peroxidation Processes

To assess the nature of lipid peroxidation in the different cell death phenotypes described above, we used the ROS-mediated lipid peroxidation characteristics described in Figure 2B and the recently established oxylipin-profiling methodology, which is based on analysis of the HOTE isomer distribution (Montillet et al., 2004). This profiling method allows discrimination between LOX-dependent and ROS-mediated lipid peroxidation in plant tissues.

A 7-h intense light exposure (1,000 $\mu$mol $m^{-2}$ $s^{-1}$ fluence rate) leads to cell death in Cat1AS leaves within 24 h (see above). This cell death is not accompanied by an intense accumulation of HFAs (Fig. 3A) and similar results were also obtained by the infiltration of the NO donor SNP (Fig. 3B). In both cases, the lipid peroxidation level increased to maximum twice, as compared to controls, but never exceeded 0.5 $\mu$mol $g^{-1}$ DW. These levels are low compared to those observed in oxidative and HR cell death (see above and below). Oxylipin profiling was done similarly on cryptogein-elicited wild-type leaves following either a continuous light, a day/night (12/12), or a night/day (12/12) regime at HL and compared to the dark situation (see above; Fig. 1, H and I). Results from the two oldest leaves, showing marked death symptoms, revealed that, for all light conditions, total lipid peroxidation levels increased (at least to 1.1 $\mu$mol $g^{-1}$ DW; Fig. 3C), as compared to mock-treated leaves (0.2 $\mu$mol $g^{-1}$ DW); however, the increase is much less than that in the dark (3.7 $\mu$mol $g^{-1}$ DW). In the light, the ROS-mediated process was mainly observed, whereas 9-LOX-dependent lipid peroxidation prevailed during complete darkness (Fig. 3C). Chiral analyses of the individual HFAs were confirmatory; whereas the 9-isomers of cryptogein-treated leaves exhibited 90% (*S*)-enantiospecificity in the dark, they were only partly chiral with an (*S*)-enantiomer composition around 63% in the light (Table I).

Taken together, these results show that (1) a ROS-mediated membrane lipid peroxidation can be correlated with cell death in response to sustained $H_2O_2$ stress in HL-treated Cat1AS plants and after administration of high levels of $H_2O_2$ in a light-driven process; (2) lipid peroxidation is minor during cell death induced in response to short $H_2O_2$ pulses or following the application of a NO donor; and (3) in cryptogein-elicited leaves, the 9-LOX-dependent lipid peroxidation occurring in the dark is almost completely inhibited by HL and, when elicitor-driven HR symptoms develop in the light, a ROS-mediated lipid peroxidation is functioning, thus suggesting a key role for $H_2O_2$ in cell death.

### Cryptogein Action on Leaves of Cat1AS Plants and Light Effects Reveal the Respective Roles of Fatty Acid Hydroperoxides and $H_2O_2$ in the Execution of HR Cell Death

In order to directly investigate the respective roles of 9-LOX metabolism and $H_2O_2$ in the execution of cell death, we compared the effect of cryptogein on cell death events under dark and HL conditions in wild-type and Cat1AS plants. In the light, we additionally compared the effects of ambient and high $CO_2$

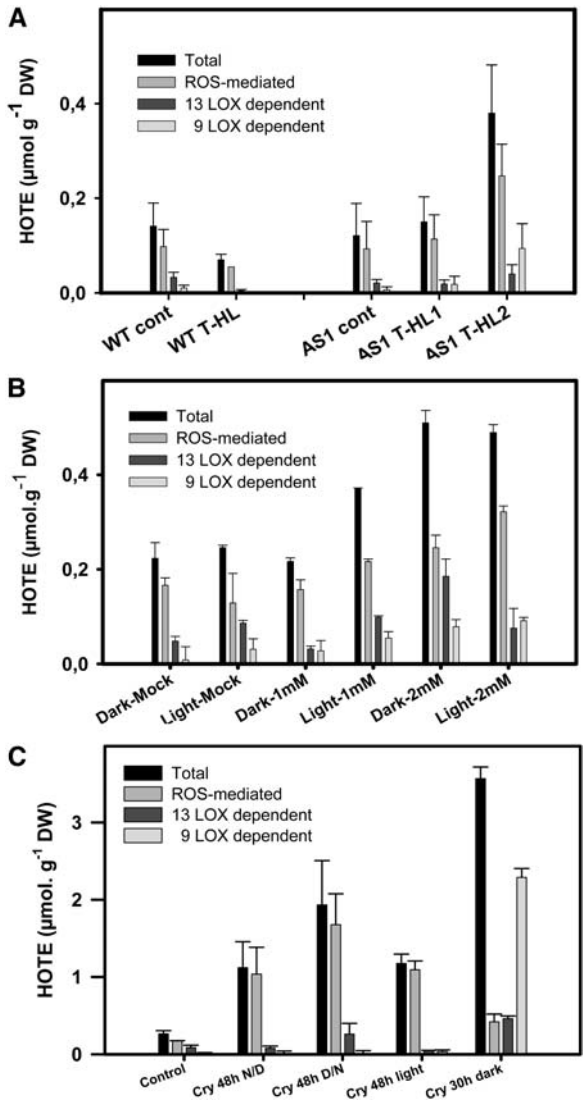


**Figure 3.** Lipid peroxidation in tobacco leaves undergoing HR-like and HR symptoms induced by transient HL or NO and cryptogein (Cry). Lipid peroxidation was investigated according to the methodology previously described, showing total ROS-mediated, 13-LOX-, and 9-LOX-dependent lipid peroxidation (Montillet et al., 2004). A, Leaves from wild-type (WT) and Cat1AS plants were submitted at the beginning of the day period to a transient intense light (1,000 $\mu$mol $m^{-2}$ $s^{-1}$ fluence rate; 7 h), followed by a return to normal light conditions (LL; 100 $\mu$mol $m^{-2}$ $s^{-1}$ fluence rate; day/night, 14/10 h). The oxylipin signature was analyzed after 24 h of incubation. Wild type and AS1 T-HL represented leaves submitted to the transient intense light condition. For AS1 T-HL1 and AS1 T-HL2, the symptoms covered 20% to 40% and about 50% of the leaf surface, respectively. B, Leaves from wild-type plants were infiltrated with 1 to 2 mM SNP on the right side of the leaf, the left side being mock infiltrated. The infiltration was carried out 2 h after the beginning of the day and the leaves were incubated either in the dark for 24 h or at HL for 6 h (350 $\mu$mol $m^{-2}$ $s^{-1}$ fluence rate), followed by an additional 18 h in the dark. Under both conditions, necrotic areas represented at least 80% of the SNP-infiltrated leaf surface. Dark and Light indicate both conditions, Mock indicates water infiltration, and 1 to 2 mM represents SNP-infiltrated leaves at the indicated concentration. C, Lipid peroxidation was characterized from cryptogein-elicited wild-type leaves (rank 9–10; see Fig. 1I) incubated for 48 h at HL in a night/day (N/D) or a day/night (D/N) cycle (12/12), under continuous light and for 30 h in the dark. See Table I for abbreviations. Results expressed as mean ± SD. For A, $n = 7$; for B and C, $n = 3$.

concentration to modulate the $H_2O_2$ background. High $CO_2$ levels impair the accumulation of HL-induced photorespiratory $H_2O_2$ in Cat1AS plants (Willekens et al., 1997).

The development of cell death on cryptogein-treated leaves kept in the dark, done by measuring solute leakage and water loss, was similar for wild-type and Cat1AS leaves (Fig. 4, A and B). Solute leakage precedes dehydration and all leaves were fully necrotic within 24 h. In parallel, total lipid peroxidation rose similarly in wild-type and Cat1AS leaves (Fig. 4C), with a massive accumulation of 9-LOX metabolites (80%–90% of total lipid peroxidation; data not shown). These results strongly suggest that an early and massive production of fatty acid hydroperoxides is enough to trigger HR cell death in the dark (Rustérucci et al., 1999). When the same infection was done with cryptogein under continuous HL conditions, either at ambient $CO_2$ (360 ppm) or at saturating $CO_2$ levels (3,000 ppm; to inhibit photorespiratory $H_2O_2$ production), cell death was delayed in wild-type leaves. Indeed necrotic symptoms only appeared after 48 h. Oxylipin profiles, characterized on each individual leaf, coincided with necrosis development (see Supplemental Fig. 2) and are indicative of a ROS-mediated process (Fig. 5). Although the average lipid peroxidation levels were 20% lower at high $CO_2$ levels, cell death phenology in wild type was similar under both $CO_2$ conditions. Contrary to wild type, the cryptogein-treated leaves from Cat1AS plants placed under 360 ppm $CO_2$ and under continuous HL were already completely necrotic within 22 h, while mock-treated Cat1AS leaves only showed tissue bleaching along the main veins due to the HL exposure (see also Dat et al., 2003). Under saturating $CO_2$, the timing of symptom development in the cryptogein-treated Cat1AS leaves was comparable to that observed under ambient $CO_2$ conditions, but the symptoms were much less developed (10%–20%; see Supplemental Fig. 2). In addition, the oxylipin profiles after 22 h of cryptogein-treated Cat1AS plants under high $CO_2$ levels revealed a 3-fold decrease of total HFA levels (Fig. 5). Taken together, these findings clearly show that, in Cat1AS leaves treated with cryptogein, the increased photorespiratory $H_2O_2$ levels are able to accelerate and/or aggravate the effect of the oxidative burst in the execution of cell death, in correlation with lipid peroxidation. In all cases, a ROS-mediated process is mainly observed (Fig. 5). Chiral analyses of individual HFAs confirmed this result (Table I) and showed that the 9-LOX-dependent process occurs at levels not exceeding 10% to 15% of total lipid peroxidation.

Taken together, these experiments strongly suggest that, in cryptogein-elicited leaves, the 9-oxylipin pathway operates efficiently in the dark, leading to a rapid

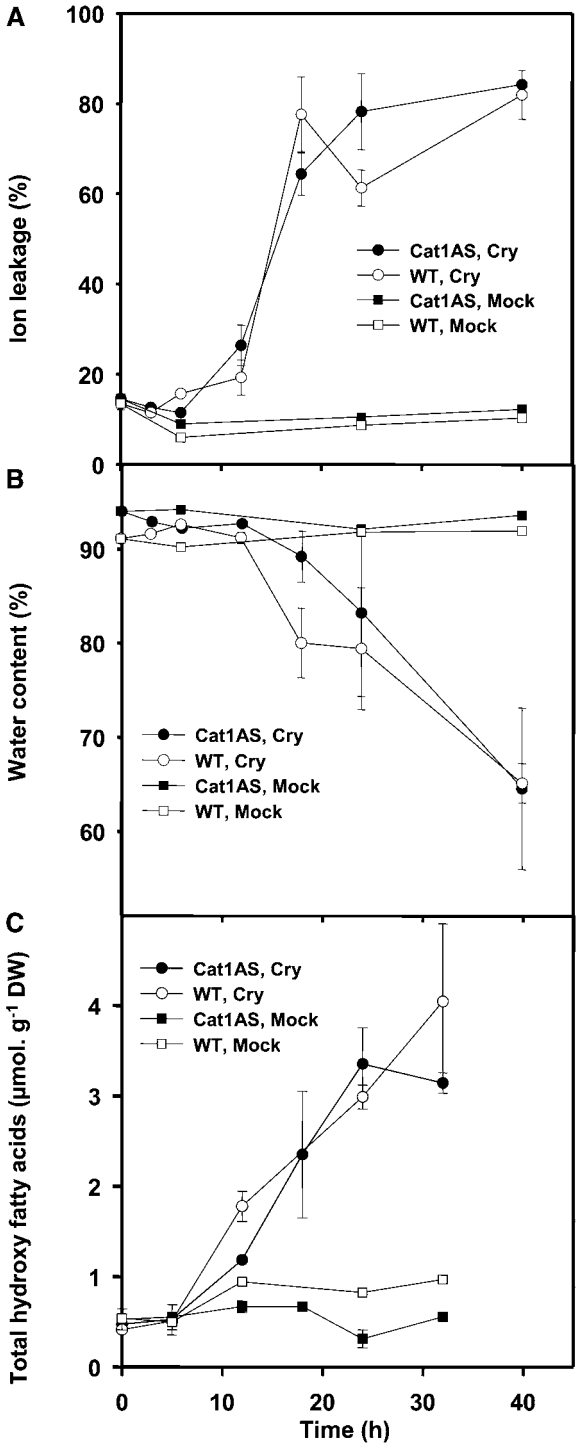


**Figure 4.** Comparison of cryptogein (Cry)-induced development of HR symptoms in the dark on detached leaves of wild-type (WT) and catalase-deficient transgenic (Cat1AS) plants. A, Solute leakage from leaf discs. B, Leaf dehydration. C, Total lipid peroxidation. See "Materials and Methods" for conditions. Results are expressed as mean ± SD from three independent experiments.

cell death, whereas in the light this pathway is impaired, revealing the participation of $H_2O_2$ in the execution of cell death.

### Both ROS- and 9-LOX-Mediated Lipid Peroxidation Occur in Response to the Avirulent Pathogen *P. syringae* pv *syringae*

In order to get further insight into the interplay between light and oxidative stress during the HR upon pathogen infection, we extended the cryptogein studies to an avirulent tobacco pathogen. Therefore, we infected wild-type and Cat1AS leaves of plants grown at LL with *P. syringae* pv s*yringae* under either a day/night regime at HL or complete darkness.

For the day/night experiment, pathogens were infiltrated ($5 \times 10^7$ cfu $mL^{-1}$ in $MgCl_2$ 10 mM) at the start of the day period. In both wild-type and Cat1AS-infected leaves, cell death led to complete tissue

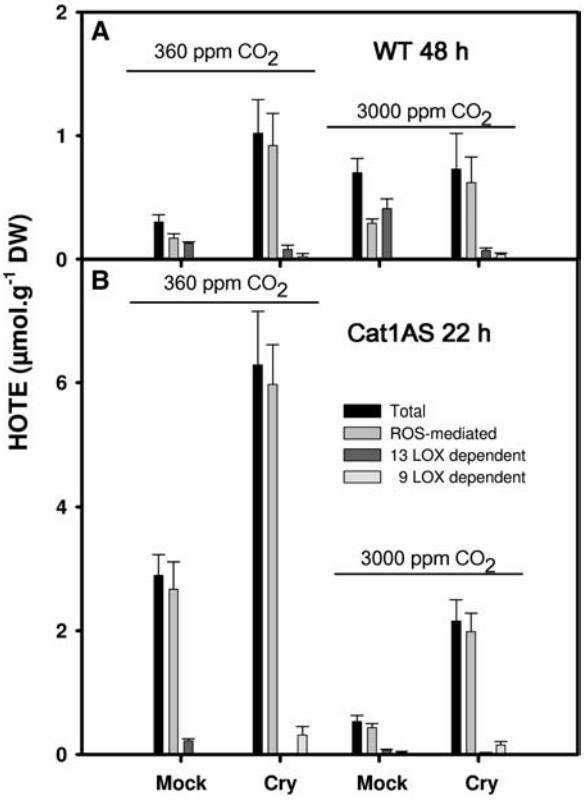


**Figure 5.** Lipid peroxidation of wild-type (WT) and catalase-deficient transgenic (Cat1AS) tobacco leaves treated with cryptogein and exposed to continuous HL under low and high $CO_2$ conditions. Detached leaves from wild-type (A) and Cat1AS (B) plants were placed into a closed chamber under continuous HL (350 $\mu$mol $m^{-2}$ $s^{-1}$ fluence rate) under normal (360 ppm) or at high (3,000 ppm) $CO_2$ conditions in order to inhibit photorespiration. The upstream oxylipin profile was determined for individual control leaves and elicited leaves undergoing HR symptoms, after 22 h for Cat1AS and 48 h for wild type (see Supplemental Fig. 2 for individual leaf analyses); see Figure 3 for lipid peroxidation characterization. Results are expressed as mean ± SD. For controls, $n = 3$; for cryptogein-elicited leaves, $n = 6$ to 9.

dehydration within 24 and 48 h for Cat1AS and wild-type leaves, respectively. Assessment of the upstream oxylipin profile revealed that, in both wild-type and Cat1AS plants, total lipid peroxidation of 18:3 increased 5 to 7 times as compared to mock-treated plants within 24 h (Fig. 6A). This increase is due in part to 9-LOX-dependent lipid peroxidation, which represents 31% and 50% of total peroxidation for wild-type and Cat1AS leaves, respectively. After 48 h, however, ROS-mediated lipid peroxidation prevailed in the wild-type leaves. In the dark, symptoms were fully developed within 24 h, and Cat1AS leaves were fully desiccated, whereas dehydration in wild-type leaves was lower. Total lipid peroxidation of 18:3 increased 10-fold for wild-type and 30-fold for Cat1AS plants (Fig. 6B). The process shows an important 9-LOX-dependent lipid peroxidation, representing 65% to 75% of the increase in the wild-type and close to 90% in Cat1AS leaves. Further insight into 9-LOX involvement in HR development was obtained with the chiral phase HPLC analysis of the HFA isomers of wild-type leaves. Interestingly, both in the day/night cycle and in the dark, Pseudomonas infection led to the production of (9*S*)-HODE and (9*S*)-HOTE (Table II), in addition to the basal levels of (13*S*)-LOX activity in mock- and pathogen-infiltrated wild-type leaves. Consistent with our previous analysis, the enantioselectivity is bigger in the dark condition [88% for (9*S*)-HOTE] than during a day/night cycle [from 81% at 24 h to 66% at 48 h for (9*S*)-HOTE], thus demonstrating the early onset of a (9*S*)-LOX-dependent peroxidation pathway following Pseudomonas infection, together with a light-driven ROS-mediated process that prevails over time in the light.

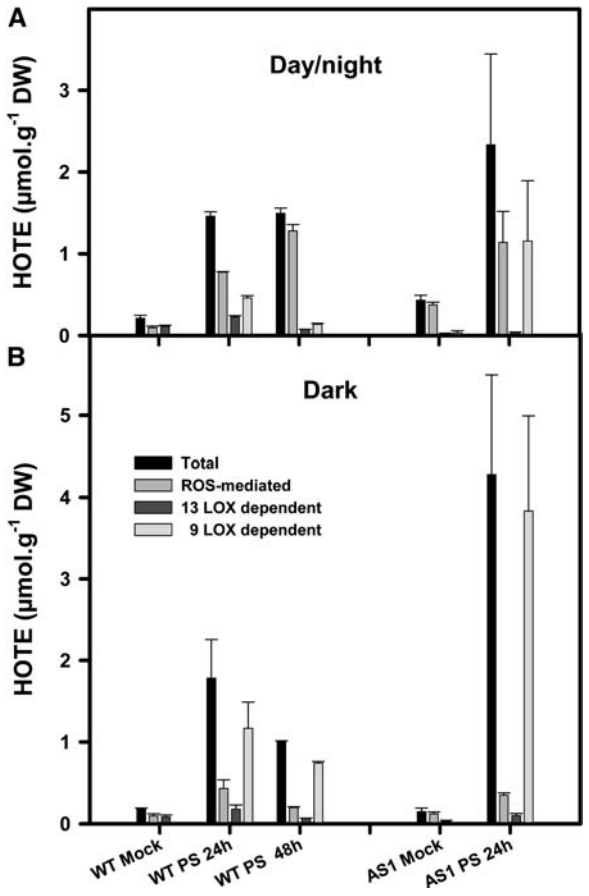


**Figure 6.** Comparison of lipid peroxidation in *P. syringae* pv *syringae*-infected leaves of wild-type (WT) and catalase-deficient transgenic (Cat1AS) plants. Leaves from plants grown at LL (100 $\mu$mol $m^{-2}$ $s^{-1}$ fluence rate; day/night, 14/10 h) were infiltrated with *P. syringae* pv *syringae* ($5 \times 10^7$ cfu $mL^{-1}$ in 10 mM $MgCl_2$) and incubated in (A) HL (350 $\mu$mol $m^{-2}$ $s^{-1}$ fluence rate; day/night, 14/10 h) or (B) the dark. The upstream oxylipin profile of Pseudomonas-inoculated leaves was determined after 24 h of incubation for wild type (WT PS 24 h) and Cat1AS (AS1 PS 24 h) plants and also after 48 h for wild-type (WT PS 48 h) plants; $MgCl_2$-inoculated leaves were included as controls and analyzed after 24 h of incubation (WT Mock and AS1 Mock). See Figure 3 for lipid peroxidation characterization. Results expressed as mean ± SD ($n = 3$).

## DISCUSSION

To assess the relative contribution and potential interdependence of $H_2O_2$ and fatty acid hydroperoxides during the execution of HR cell death, we investigated lipid peroxidation processes involved during various model conditions inducing cell death in tobacco leaves. We showed that cell death triggered by both $H_2O_2$ infiltration and a sustained photorespiratory-induced $H_2O_2$ stress in Cat1AS plants is associated with an intense free radical-mediated lipid peroxidation of membranes. We also established that a short pulse of HL in Cat1AS leaves triggers cell death without massive lipid peroxidation. Similar results were also obtained when infiltrating a NO donor. From these initial results, it was concluded that (1) lipid peroxidation does not always accompany cell death processes; (2) increased $H_2O_2$ and NO levels trigger only part of the HR cell death processes; and (3) the combination of light and massive $H_2O_2$ production is necessary to provoke an intense ROS-mediated lipid peroxidation.

To characterize in more detail the different cell death processes, we used a methodology that distinguishes between 9-LOX-, 13-LOX-, and ROS-mediated lipid peroxidation processes (Montillet et al., 2004). We showed previously that, in the dark, the HR in tobacco is characterized by the induction of the 9-oxylipin metabolism (Rustérucci et al., 1999) and that this process can be inhibited by light (Cacas et al., 2005). In this work, we show that, under various light conditions, the cryptogein-induced HR is (1) inhibited in young, fully developed leaves but not in the older leaves of the plant; (2) not dependent on the timing of the elicitation under a day/night cycle; and (3) mainly characterized by a ROS-mediated lipid peroxidation. Thus, by comparing the lipid peroxidation characteristics of cryptogein-induced HR in the dark and in the light, both in wild-type and Cat1AS plants, we were able to investigate the role of $H_2O_2$ in HR cell death.

**Table II.** *Enantioselectivity in lipid peroxidation induced by pathogen infection*

Enantiomer composition of the HFAs obtained by the $NaBH_4$/hydrolysis procedure from control, *P. syringae*-infiltrated wild-type leaves. Same conditions as in Figure 6. Results are expressed as mean ± SD ($n = 2$). 9-HODE, 9-hydroxy-10,12(*E*,*Z*) octadecadienoic acid; 13-HODE, 13-hydroxy-9,11(*Z*,*E*) octadecadienoic acid; 9-HOTE, 9-hydroxy-10,12,15(*E*,*Z*,*Z*) octadecatrienoic acid; 12-HOTE, 12-hydroxy-9,13,15(*Z*,*E*,*Z*)-octadecatrienoic acid; 13-HOTE, 13-hydroxy-9,11,15(*Z*,*E*,*Z*)-octadecatrienoic acid; 16-HOTE, 16-hydroxy-9,12,14(*Z*,*Z*,*E*)-octadecatrienoic acid.

| HFAs | (*S*)-Enantiomer (%) | | | | |
|---|---|---|---|---|---|
| | $MgCl_2$ HL, 24 h (Day/Night, 14/10 h) | Pseudomonas Dark, 24 h | Pseudomonas Dark, 48 h | Pseudomonas HL, 24 h (Day/Night, 14/10 h) | Pseudomonas HL, 48 h (Day/Night, 14/10 h) |
| 9-HODE | 49 ± 0 | 88 ± 1 | 88 ± 1 | 75 ± 1 | 58 ± 1 |
| 9-HOTE | 49 ± 0 | 88 ± 1 | 87 ± 2 | 81 ± 2 | 66 ± 1 |
| 13-HODE | 77 ± 2 | 68 ± 1 | 62 ± 1 | 59 ± 1 | 53 ± 1 |
| 13-HOTE | 93 ± 5 | 71 ± 1 | 65 ± 1 | 73 ± 1 | 55 ± 1 |
| 12-HOTE | 54 ± 1 | 50 ± 1 | 51 ± 1 | 56 ± 2 | 51 ± 1 |
| 16-HOTE | 47 ± 3 | 48 ± 1 | 48 ± 1 | 49 ± 2 | 49 ± 1 |

Under dark conditions, the development of cryptogein-induced HR was identical in both Cat1AS and wild-type leaves and the lipid peroxidation was characterized by the same massive production of the 9-LOX products. Thus, $H_2O_2$ detoxification by catalase is not essential for symptom development in the dark, and $H_2O_2$ is not involved as a signal in the induction of the 9-oxylipin pathway. Furthermore, our results also suggest that $H_2O_2$ produced by the oxidative burst in the dark does not play an important role in the execution of cell death, but that an early and massive production of fatty acid hydroperoxides has a more prominent role in this execution. Under continuous light conditions, we have observed that (1) the cell death symptoms (if not completely blocked in fully developed young leaves), which are correlated with the increase in lipid peroxidation levels, are delayed in comparison to the dark situation; (2) the main lipid peroxidation process is mediated by the production of $H_2O_2$, whereas 9-LOX metabolism is low; (3) when catalase activity is decreased (Cat1AS plants), the effect of $H_2O_2$ is amplified leading both to earlier development of symptoms and to increased ROS-mediated lipid peroxidation; and (4) under high $CO_2$, in Cat1AS leaves, both symptoms and ROS-mediated lipid peroxidation are decreased, showing that photorespiratory $H_2O_2$ participates here in cell death execution. Taken together, these results show that the production of both fatty acid hydroperoxides and $H_2O_2$ occurs in tobacco HR and can be considered as participants in the execution of HR cell death.

Oxylipin metabolism in the dark involves the induction of galactolipase and 9-LOX activities, respectively (Cacas et al., 2005). This metabolism can be induced early after pathogen assault, operates within 24 h, and is sufficient for the development of HR symptoms. During cryptogein elicitation in the light, this oxylipin pathway is inhibited at the transcriptional level. Under those conditions, the light-driven increase in $H_2O_2$ levels leads to ROS-mediated peroxidation of the membranes in a later phase. Since this ROS-mediated lipid peroxidation is closely correlated to cell death symptoms, and since these two processes occur earlier, are more pronounced, and are also inhibited partly under high $CO_2$ in cryptogein-elicited Cat1AS leaves, it can be argued that $H_2O_2$ plays a direct role in the execution of cell death. The fact that $H_2O_2$-detoxifying enzyme activities, catalase, and cytosolic ascorbate peroxidase decline during the development of HR in leaves (Dorey et al., 1998; Mittler et al., 1998) consolidates our observations. Interestingly, in the infection by the incompatible pathogen *P. syringae* pv *syringae*, our results indicate that 9-LOX metabolism and $H_2O_2$ production are both involved in the HR process.

$H_2O_2$ is known to play different roles in the HR (Doke, 1997; Lamb and Dixon, 1997; Grant and Loake, 2000). It contributes to cell wall reinforcement, limiting pathogen spread, and it can also directly participate in pathogen killing. For example, in tobacco, the modulation of catalase activity by antisense technology leads to more resistant plants against pathogen attack (Mittler et al., 1999), whereas overproduction leads to more sensitive plants (Polidoros et al., 2001; Talarczyk et al., 2002). $H_2O_2$ was shown to initiate a cell death program in Arabidopsis plants and suspension cultures (Desikan et al., 1998; Vandenabeele et al., 2004), in tobacco BY-2 cells (Houot et al., 2001), and in Cat1AS tobacco plants exposed to HL to activate a cell death process that involves the activation of an oxidative burst (Dat et al., 2003). Here, we show that $H_2O_2$ can also be involved in late execution during HR programmed cell death via light-dependent membrane lipid peroxidation. To explain the role of light, it might be argued that the Fenton reaction, leading to $HO^{\cdot}$ production from $H_2O_2$ and thus to lipid peroxidation, needs a cyclic reduction of $Fe^{3+}$ into $Fe^{2+}$ (Halliwell and Gutteridge, 2000). This process can be achieved by a light-driven recycling of redox compounds such as ascorbate. Additionally, the free fatty acid hydroperoxides that are produced enzymatically can also be substrates of Fenton-like reactions, leading, similarly, to the production of alkoxy radicals (Halliwell and Gutteridge, 2000) and thus enhancing the free radical-mediated lipid peroxidation in the light.

Investigation of the light effect in plant pathogen interactions is only in its infancy (Karpinski et al., 2003). In Arabidopsis, a light-signaling pathway was

shown to interact with the salicylic acid-mediated signal transduction pathway and necessary to trigger the HR response to pathogens (Genoud et al., 2002; Zeier et al., 2004). Additionally, in the *lsd1* mutant, the runaway cell death, but not the initial HR after *Pseudomonas parasitica* inoculation, was shown to be dependent on light and to involve photorespiratory $H_2O_2$ production (Mateo et al., 2004). More specifically, light-mediated leaf cell redox homeostasis and antioxidant cross-talk between mitochondria and the other organelles was shown to be essential in plant resistance to tobacco mosaic virus (Dutilleul et al., 2003). In tobacco cells, the involvement of redox status change of ascorbate and glutathione was proposed as part of the signaling pathways leading to programmed cell death (de Pinto et al., 2002). Redox regulation of transcription factors in eukaryotes was initially demonstrated in yeast (*Saccharomyces cerevisiae*; Delaunay et al., 2002), while NPR1, a key transcriptional regulator of plant systemic acquired resistance, is under redox control (Mou et al., 2003). In cryptogein-elicited leaves, the light effect on the inhibition of the 9-oxylipin pathway might be related to such redox regulation. However, if in the elicited material this metabolism can be switched off, keeping a place for $H_2O_2$-involved HR cell death, in the case of pathogen infection the response is composite. Indeed, in Pseudomonas-infected leaves, under normal light conditions, the ROS-mediated lipid peroxidation appears as the main process but, in addition, the activation of the 9-oxylipin pathway also leads to a massive accumulation of (9*S*) fatty acid hydroperoxides (30%–50% of total lipid peroxidation). Such a production might be at the origin of signaling and death processes involving reactive electrophile species (Farmer et al., 2003). Many aspects of the light response remain to be elucidated and, in this way, the cryptogein model might help in the characterization of the key factors involved in the induction/regulation of the 9-oxylipin pathway leading to the massive production of fatty acid hydroperoxides.

Besides both types of hydroperoxide production, many other parallel processes, such as the activation of nucleases and proteases, are involved in HR cell death execution. The fact that different effectors of cell death can operate independently also provides the plant with a diverse scala of strategies to execute different and specific types of cell death (e.g. during pathogen and developmentally driven cell death processes; Heath, 2000).

## MATERIALS AND METHODS

### Plant Material and Treatments

Cat1AS is a transgenic line of tobacco (*Nicotiana tabacum*) cv Petit Havana SR1 with approximately 10% of wild-type catalase activity (Chamnongpol et al., 1996). Cat1AS and control wild-type plants (SR1) were precultivated under LL (100 ± 20 $\mu$mol $m^{-2}$ $s^{-1}$ fluence rate; day/night, 14/10 h) at 25°C and 70% relative humidity. Mature preflowering plants (6–8 weeks old) were used for all experiments. Otherwise stated, HL treatment consisted of 350 ± 50 $\mu$mol $m^{-2}$ $s^{-1}$ fluence rate, with the selected lightning cycle. $H_2O_2$ (1 M) or SNP (1 or 2 mM) treatments were carried out by infiltration, applying the syringe tip to the epidermis of the leaves.

For the elicitation experiments, leaves were detached from the plants and treated at the petiole with 10 $\mu$L of an aqueous solution of cryptogein (0.2 $\mu$g $\mu L^{-1}$), followed after absorption by 3 × 10 $\mu$L of water. Control leaves were treated similarly with water. The leaves were then placed horizontally into a couple of closed chambers and watered by the petiole. A couple of chambers allow controlled lighting, humidity (70%), and the capacity to simultaneously carry out the experiments under low and high $CO_2$ atmosphere (360 or 3,000 ppm).

Plants were maintained at LL (day/night, 14/10 h) before pathogen infection. For induction of the HR, 5 × $10^7$ cfu $mL^{-1}$ of *Pseudomonas syringae* pv *syringae* in 10 mM $MgCl_2$ was inoculated by leaf infiltration (Chamnongpol et al., 1996), 50% to 75% of the leaf surface being infiltrated with the bacteria. The Pseudomonas-infected wild-type plants were maintained either in the dark or at HL (day/night, 14/10 h). Mock-infiltrated plants (10 mM $MgCl_2$) were used for controls.

### Lipid Peroxidation Analyses

Total free and esterified hydroxy and hydroperoxy fatty acids were analyzed by HPLC as free HFAs, after $NaBH_4$ reduction and hydrolysis, as described previously (Rustérucci et al., 1999; Montillet et al., 2004).

Solute leakage was determined by measuring the conductivity change of pure water (5 mL; 18 MΩ) after 2-h incubation of five leaf discs (diameter 9 mm), as referred to the conductivity at equilibrium.

### Microscopic Analysis of Phenotypes

For sectioning, fresh plant material was fixed in formaldehyde (5%), acetic acid (5%), and alcohol (45%), and passed over a graded ethanol series. Infiltration and embedding in Historesin (7022–18500 Leica Historesin embedding kit; Leica Microsystems, Heidelberg) were performed according to the manufacturer's instructions. Sections (5–10 $\mu$m) were cut on a rotary microtome (Minot-Milerotonn 1212; Leitz, Wetzlar, Germany) with disposable Superlab Knifes (Adamas Instrumenten, Leersum, The Netherlands). Morphological sections of leaves were stained with 0.05% toluidine blue for 10 min before examination under a light microscope.

## ACKNOWLEDGMENTS

We thank the GRAP team (CEA/Cadarache, DSV-DEVM) for technical support in plant culture and experiments in closed chambers, Stijn Morsa for excellent technical assistance, and Céline Davoine for reading and editing the manuscript.

Received January 19, 2005; revised April 13, 2005; accepted April 25, 2005; published June 24, 2005.

## LITERATURE CITED

**Beers EP, McDowell JM** (2001) Regulation and execution of programmed cell death in response to pathogens, stress and developmental cues. Curr Opin Plant Biol **4:** 561–567

**Cacas JL, Vailleau F, Davoine C, Ennar N, Agnel JP, Tronchet M, Ponchet M, Blein JP, Roby D, Triantaphylidès C, et al** (2005) The combined action of 9 lipoxygenase and galactolipase is sufficient to bring about programmed cell death during tobacco hypersensitive response. Plant Cell Environ **28:** (in press)

**Chamnongpol S, Willekens H, Langebartels C, Van Montagu M, Inzé D, Van Camp W** (1996) Transgenic tobacco with a reduced catalase activity develops necrotic lesions and induces pathogenesis-related expression under high light. Plant J **10:** 491–503

**Chamnongpol S, Willekens H, Moeder W, Langebartels C, Sanderman H, Van Montagu M, Inzé D, Van Camp W** (1998) Defense activation and enhanced pathogen tolerance induced by $H_2O_2$ in transgenic tobacco. Proc Natl Acad Sci USA **95:** 5818–5823

**Dat JF, Inzé D, Van Breusegem F** (2001) Catalase-deficient tobacco plants: tools for in planta studies on the role of hydrogen peroxide. Redox Rep **6:** 37–42

**Dat JF, Pellinen R, Beeckman T, van de Cotte B, Langebartels C, Kangasjarvi J, Inzé D, Van Breusegem F** (2003) Changes in hydrogen peroxide homeostasis trigger an active cell death process in tobacco. Plant J **33:** 621–632

**Degousée N, Triantaphylidès C, Starek S, Iacazio G, Martini D, Bladier C, Voisine R, Montillet JL** (1995) Measurement of thermally produced volatile alkanes: an assay for plant hydroperoxy fatty acid evaluation. Anal Biochem **224:** 524–531

**Delaunay A, Pflieger D, Barrault MB, Vinh J, Toledano MB** (2002) A thiol peroxidase is an $H_2O_2$ receptor and redox-transducer in gene activation. Cell **111:** 471–481

**Delledonne M, Zeier J, Marocco A, Lamb C** (2001) Signal interactions between nitric oxide and reactive oxygen intermediates in the plant hypersensitive disease resistance response. Proc Natl Acad Sci USA **98:** 13454–13459

**de Pinto MC, Tommasi F, De Gara L** (2002) Changes in the antioxidant systems as part of the signaling pathway responsible for the programmed cell death activated by nitric oxide and reactive oxygen species in tobacco Bright-Yellow 2 cells. Plant Physiol **130:** 698–708

**Desikan R, Reynolds A, Hancock JT, Neill SJ** (1998) Harpin and hydrogen peroxide both initiate programmed cell death but have differential effects on defence gene expression in Arabidopsis suspension cultures. Biochem J **330:** 115–120

**Doke N** (1997) The oxidative burst: roles in signal transduction and plant stress. *In* JG Scandalios, ed, Oxidative Stress and the Molecular Biology of Antioxidant Defenses. Cold Spring Harbor Laboratory Press, Cold Spring Harbor, New York, pp 785–813

**Dorey S, Baillieul F, Saindrenan P, Fritig B, Kauffmann S** (1998) Tobacco class I and II catalases are differentially expressed during elicitor-induced hypersensitive cell death and localized acquired resistance. Mol Plant-Microbe Interact **11:** 1102–1109

**Dutilleul C, Garmier M, Noctor G, Mathieu C, Chetrit P, Foyer CH, de Paepe R** (2003) Leaf mitochondria modulate whole cell redox homeostasis, set antioxidant capacity, and determine stress resistance through altered signaling and diurnal regulation. Plant Cell **15:** 1212–1226

**Farmer EE, Almeras E, Krishnamurthy V** (2003) Jasmonates and related oxylipins in plant responses to pathogenesis and herbivory. Curr Opin Plant Biol **6:** 372–378

**Genoud T, Buchala AJ, Chua NH, Métraux JP** (2002) Phytochrome signalling modulates the SA-perceptive pathway in *Arabidopsis.* Plant J **31:** 87–95

**Grant JJ, Loake GJ** (2000) Role of reactive oxygen intermediates and cognate redox signaling in disease resistance. Plant Physiol **124:** 21–29

**Greenberg JT, Yao N** (2004) The role and regulation of programmed cell death in plant-pathogen interactions. Cell Microbiol **6:** 201–211

**Halliwell B, Gutteridge JMC** (2000) Free Radicals in Biology and Medicine, Ed 3. Clarendon Press, Oxford

**Heath MC** (2000) Hypersensitive response-related cell death. Plant Mol Biol **44:** 321–334

**Houot V, Etienne P, Petitot AS, Barbier S, Blein JP, Suty L** (2001) Hydrogen peroxide induces programmed cell death features in cultured tobacco BY-2 cells, in a dose-dependent manner. J Exp Bot **52:** 1721–1730

**Jalloul A, Montillet JL, Assigbetsé K, Agnel JP, Delannoy E, Triantaphylidès C, Daniel JF, Marmey P, Geiger JP, Nicole M** (2002) Lipid peroxidation in cotton: *Xanthomonas* interactions and the role of lipoxygenases during the hypersensitive reaction. Plant J **32:** 1–12

**Karpinski S, Gabrys H, Mateo A, Karpinska B, Mullineaux PM** (2003) Light perception in plant disease defence signalling. Curr Opin Plant Biol **6:** 390–396

**Knight VI, Wang H, Lincoln JE, Lulai EC, Gilchrist DG, Bostock RM** (2001) Hydroperoxides of fatty acids induce programmed cell death in tomato protoplasts. Physiol Mol Plant Pathol **59:** 277–286

**Lam E** (2004) Controlled cell death, plant survival and development. Nat Rev Mol Cell Biol **5:** 305–315

**Lamb C, Dixon RA** (1997) The oxidative burst in plant disease resistance. Annu Rev Plant Physiol Plant Mol Biol **48:** 251–275

**Maccarone M, Van Zadelhoff G, Veldink GA, Vliengenthart JFG, Finazzi-Agro A** (2000) Early activation of lipoxygenase in lentil (*Lens culinaris*) root protoplasts by oxidative stress induces programmed cell death. Eur J Biochem **267:** 5078–5084

**Martin GM, Bogdanove AJ, Sessa G** (2003) Understanding the functions of plant disease resistance proteins. Annu Rev Plant Biol **54:** 23–61

**Mateo A, Muhlenbock P, Rusterucci C, Chang CC, Miszalski Z, Karpinska B, Parker JE, Mullineaux PM, Karpinski S** (2004) LESION SIMULATING DISEASE 1 is required for acclimation to conditions that promote excess excitation energy. Plant Physiol **136:** 2818–2830

**Mittler R, Feng X, Cohen M** (1998) Post-transcriptional suppression of cytosolic ascorbate peroxidase expression during pathogen-induced programmed cell death in tobacco. Plant Cell **10:** 461–473

**Mittler R, Herr EH, Orvar BL, Van Camp W, Willekens H, Inzé D, Ellis BE** (1999) Transgenic tobacco plants with reduced capability to detoxify reactive oxygen intermediates are hyperresponsive to pathogen infection. Proc Natl Acad Sci USA **96:** 14165–14170

**Montillet JL, Agnel JP, Ponchet M, Vailleau F, Roby D, Triantaphylidès C** (2002) Lipoxygenase-mediated production of PUFA hydroperoxydes is a specific signature of the hypersensitive reaction in plants. Plant Physiol Biochem **40:** 633–639

**Montillet JL, Cacas JL, Garnier L, Montané MH, Douki T, Bessoule JJ, Polkowska-Kowalczyk L, Maciejewska U, Agnel JP, Vial A, et al** (2004) The upstream oxylipin profile of *Arabidopsis thaliana*. A tool to scan for oxidative stresses. Plant J **40:** 439–451

**Mou Z, Fan W, Dong X** (2003) Inducers of plant systemic acquired resistance regulate NPR1 function through redox changes. Cell **113:** 935–944

**Neill SJ, Desikan R, Clarke A, Hurst RD, Hancock JT** (2002) Hydrogen peroxide and nitric oxide as signalling molecules in plants. J Exp Bot **53:** 1237–1247

**Polidoros AN, Mylona PV, Scandalios JG** (2001) Transgenic tobacco plants expressing the maize Cat2 gene have altered catalase levels that affect plant-pathogen interactions and resistance to oxidative stress. Transgenic Res **10:** 555–569

**Rancé I, Fournier J, Esquerré-Tugayé MT** (1998) The incompatible interaction between *Phytophthora parasitica* var. *nicotianae* race 0 and tobacco is suppressed in transgenic plants expressing antisense lipoxygenase sequences. Proc Natl Acad Sci USA **95:** 6554–6559

**Rathjen JP, Moffett P** (2003) Early signal transduction events in specific plant disease resistance. Curr Opin Plant Biol **6:** 300–306

**Rustérucci C, Montillet JL, Agnel JP, Battesti C, Alonso B, Knoll A, Bessoule JJ, Etienne P, Suty L, Blein JP, et al** (1999) Involvement of lipoxygenase-dependent production of fatty acid hydroperoxides in the development of the hypersensitive cell death induced by cryptogein on tobacco leaves. J Biol Chem **274:** 36446–36455

**Simon-Plas F, Rustérucci C, Milat ML, Humbert C, Montillet JL, Blein JP** (1997) Active oxygen species production in tobacco cells elicited by cryptogein. Plant Cell Environ **20:** 1573–1579

**Talarczyk A, Krzymowska M, Borucki W, Hennig J** (2002) Effect of yeast CTA1 gene expression on response of tobacco plants to tobacco mosaic virus infection. Plant Physiol **129:** 1032–1044

**Vailleau F, Daniel X, Tronchet M, Montillet JL, Triantaphylidès C, Roby D** (2002) A R2R3-MYB gene, *AtMYB30*, acts as a positive regulator of the hypersensitive cell death program in plants in response to pathogen attack. Proc Natl Acad Sci USA **99:** 10179–10184

**Vandenabeele S, Van Der Kelen K, Dat J, Gadjev I, Boonefaes T, Morsa S, Rottiers P, Slooten L, Van Montagu M, Zabeau M, et al** (2003) A comprehensive analysis of hydrogen peroxide-induced gene expression in tobacco. Proc Natl Acad Sci USA **100:** 16113–16118

**Vandenabeele S, Vanderauwera S, Vuylsteke M, Rombauts S, Langebartels C, Seidlitz HK, Zabeau M, Van Montagu M, Inzé D, Van Breusegem F** (2004) Catalase deficiency drastically affects high light-induced gene expression in *Arabidopsis thaliana.* Plant J **39:** 45–58

**Wendehenne D, Durner J, Klessig DF** (2004) Nitric oxide: a new player in plant signalling and defense responses. Curr Opin Plant Biol **7:** 449–455

**Willekens H, Chamnongpol S, Davey M, Schraudner M, Langebartels C, Van Montagu M, Inzé D, Van Camp W** (1997) Catalase is a sink for $H_2O_2$ and is indispensable for stress defense in C3 plants. EMBO J **16:** 4806–4816

**Zeier J, Pink B, Mueller MJ, Berger S** (2004) Light conditions influence specific defence responses in incompatible plant-pathogen interactions: uncoupling systemic resistance from salicylic acid and PR-1 accumulation. Planta **219:** 673–683